Upgraded equilibrium reconstruction by coupling of an extended set of measurements with current diffusion modelling at ASDEX Upgrade

R. Fischer[1], A. Bock, A. Burckhart, M. Dunne, O. Ford, J.C. Fuchs, L. Giannone, A. Gude, V. Igochine, A. Lebschy, M. Maraschek, P.J. McCarthy, A. Mlynek, A. Snicker, J. Stober, G. Tardini, M. Weiland, M. Willensdorfer, and the ASDEX Upgrade Team

[1]*Max-Planck-Institut für Plasmaphysik, Boltzmannstr. 2, D-85748 Garching, Germany*

The omnipresent ill-posedness of tokamak equilibrium reconstructions can be mitigated by an integrated approach of combining a comprehensive set of internal and external measurements with a predictive model of the expected current distribution. The goal is to overcome the need for non-physical regularization (smoothing) of the source profiles entering the Grad-Shafranov equation by a sufficiently informative set of measurements and physical modelling. An extended set of data allows to validate their mutual compatibility due to partially redundant information.

Grad-Shafranov Equation The GSE describing an ideal magneto-hydrodynamic equilibrium in axisymmetric tokamak geometry reads

$$\left(R\frac{\partial}{\partial R}\frac{1}{R}\frac{\partial}{\partial R}+\frac{\partial^2}{\partial z^2}\right)\psi=-2\pi\mu_0 R j_\phi(\psi) \quad ; \quad j_\phi := 2\pi\left(R\frac{\partial p(\psi)}{\partial\psi}+\frac{F(\psi)}{\mu_0 R}\frac{\mathrm{d}F(\psi)}{\mathrm{d}\psi}\right), \quad (1)$$

where $\psi(R,z)$ denotes the poloidal flux function in cylindrical coordinates (R, z). The toroidal current density profile, j_ϕ, consists of two terms, where $p(\psi)$ is the plasma pressure (isotropic case) and $F(\psi)=\mu_0 I_{\mathrm{pol}}/(2\pi)$ is proportional to the total poloidal current I_{pol}.

The GSE is solved at ASDEX Upgrade subject to an extended set of constraints within an Integrated Data analysis suite with Equilibrium (IDE). Recently the 59 measurements from poloidal and radial magnetic field coils were extended by a second poloidal ring of 29 coils toroidally separated by 45 degrees. This enables to study effects of magnetic field perturbation on the plasma and the control system. A set of 18 toroidal flux loop measurements was recently supplemented by a diamagnetic flux loop measurement [1]. These magnetic measurements are complemented by measurements of divertor tile currents constraining the poloidal current in the scrape of layer and 3 loop voltage measurements, two on the low-field (lfs) and one on the high-field side (hfs). The forward model of the loop voltage measurements requires temporal correlation of successive equilibria provided anyway by the modelling constraints (see below).

Pressure profiles constraining the p'-term consists of the sum of the pressure if the thermal electrons and ions and of the fast ions. The electron thermal pressure profile is provided by the Integrated Data Analysis (IDA) suite [2]. The ion thermal pressure is calculated from the ion temperature available from charge exchange recombination spectroscopy (CXRS) on two toroidally separated neutral heating beams for full temporal coverage ($T_{\mathrm{i}}=T_{\mathrm{e}}$ is assumed

without beams) and the ion density using the electron density (IDA) and a Z_{eff} profile from either bremsstrahlung [3] or the impurity densities from CXRS. The pressure profile and neutral beam current drive (NBCD) of the fast ions are taken either from TRANSP calculations or from a recently developed method which is based on an orbit averaged beam deposition and an analytical solution of the Fokker-Planck equation, as described in sections 2.2-2.3 of [4]. The pressure constraints together with the diamagnetic flux loop measurements provide a redundant set which allows to validate the thermal and fast ion profiles. In particular in the absence of neutral beams (no T_{i} measurements) and the presence of electron cyclotron heating the assumption of $T_{\mathrm{i}} = T_{\mathrm{e}}$ might not be valid which can clearly be seen in a mismatch of the modelled and measured diamagnetic flux as well as in the fitting of the pressure constraints.

Geometrical information about flux surfaces are provided by iso-flux constraints [5] from redundant measurements of the electron temperature on the high- and low-field side. Recently an upgraded suite of CXRS diagnostics allows to exploit also ion temperature measurements assuming T_{i} being constant on flux surfaces. Iso-flux constraints are applicable if T_{e}- or T_{i}-profile gradients allow a unique allocation of flux surfaces with temperature values. This is not possible, e.g., after a sawtooth crash with flat profiles close to the plasma center.

Internal information about the current distribution is provided by spatially resolved motional stark effect (MSE) and, since recently, imaging MSE (iMSE) measurements [6]. Additionally, polarimetry measurements of two lines of sight (LOSs) provide line integrated measurements of the projected magnetic field [7]. Since the poloidally oriented LOSs have a small toroidal tilt angle, the toroidal field contribution has to be calibrated from two similar discharges with reversed toroidal field. A plausible toroidal tilt angle of about 0.4 degrees for both LOSs was estimated. Further calibration measures of the detection system is in progress. Although polarimetry is momentarily less sensitive than the iMSE, it is available throughout the plasma discharge whereas the (i)MSE has to rely on appropriate neutral beams. The current and pressure measurements in combination with the localisation of MHD modes and the presence of sawtooth crashes provide a valuable redundant set to validate individual diagnostics.

Current Diffusion Equation The extended set of heterogeneous measurements is complemented by flux-surface averaged toroidal current distributions obtained by employing the CDE (also known as poloidal flux diffusion equation) between successive equilibria,

$$\sigma_{\parallel}\frac{\partial\psi}{\partial t} = \frac{R_0 J^2}{\mu_0\rho}\frac{\partial}{\partial\rho}\left(\frac{G_2}{J}\frac{\partial\psi}{\partial\rho}\right) - \frac{V'}{2\pi\rho}(j_{\mathrm{bs}} + j_{\mathrm{nbcd}} + j_{\mathrm{eccd}}) \quad ; \quad \rho := \sqrt{\frac{\Phi}{\pi B_0}} \quad . \tag{2}$$

$\psi(\rho)$ is the poloidal magnetic flux at the toroidal flux coordinate ρ with the toroidal magnetic flux Φ and the vacuum magnetic field $B_0 = B(R_0)$ at the reference radius R_0. The CDE describes the diffusion of the poloidal flux on the background of the toroidal flux due to resistivity. The

coupling of the *predictive* CDE with the *inverse* equilibrium reconstruction from the GSE is performed in two steps. Starting with a previous equilibrium the CDE is iterated till the next time where an equilibrium is to be estimated. The flux-surface averaged toroidal current distribution from the iterated CDE provides an estimate of the GSE $\langle j_\phi \rangle$. Finally, the next equilibrium is evaluated using the GSE solver by minimising a least-squares criterion on all the measured data and modelling $\langle j_\phi \rangle$ including their uncertainties. The modelled $\langle j_\phi \rangle$ uncertainty is due to uncertainties in the various parameters entering the CDE. Details about the coupling, the geometric quantities, the bootstrap j_{bs} and driven currents from neutral beams j_{nbcd} and electron cyclotron resonance heating j_{eccd}, and the uncertainty treatment can be found in [8].

Sawtooth crash Since the CDE does not consider current redistribution events such as sawtooth crashes, additional redistribution models have to be included. The identification of a sawtooth crash can optionally be chosen from a simplified shear criterion at the $q = 1$ surface or from a sawtooth identification scheme employing soft X-ray data. Redistribution models encompass full or partial reconnection given by the Kadomtsev model or a newly employed variant based on a $q = 1$-surface conserving redistribution scheme supported by soft X-ray observations [9]. The $q = 1$-surface is conserved if the current is redistributed only within the $q = 1$-surface. The simplest approach is to redistribute the total current within the $q = 1$-surface uniformly. In contrast to the Kadomtsev model the resulting q-profile stays below one throughout the area within the $q = 1$-surface.

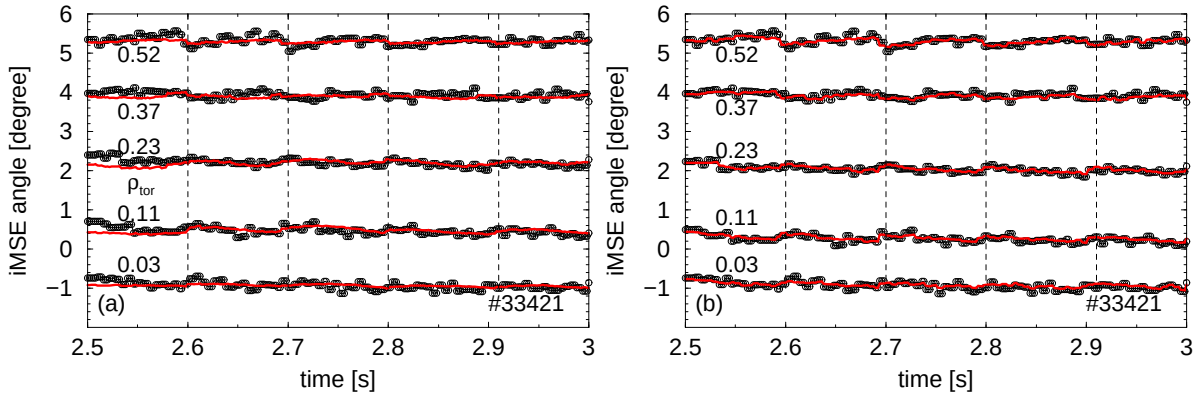

Figure 1: *Time traces of measured (circles) and modelled (red line) iMSE angles without (a) and with (b) using the angles in the equilibrium reconstruction for a sawtoothing discharge (dashed vertical lines).*

An example of equilibrium reconstruction with the upgraded suite of measurements and modelling including first iMSE measurements is shown in fig. 1 for discharge #33421 with strong sawtooth crashes (SCs). The sawtooth reconnection method with current redistribution only within the $q = 1$-surface was applied although the present data do not provide sufficient information to validate the various sawtooth models. The measured iMSE angles (circles) are compared to the modelled angles based (a) on magnetic, polarimetry and current diffusion data and (b) additionally on the iMSE angles. SC induced jumps up to 0.4 degrees can clearly be re-

solved in the measured angles. At mid-radius ($\rho_{\text{tor}} = 0.52$) and close to the center ($\rho_{\text{tor}} = 0.11$) the jumps go in opposite directions. The modelled angles without fitting the iMSE angles (a) describe the jumps reasonably well but partially with reduced size. Fitting additionally 114 iMSE angles in $1.65m < R < 2.06m$ and $-0.1m < z < 0.2m$ (b) reduces the residues significantly, as expected. The SC induced iMSE angle variation close to the magnetic axis are due to two opposite effects. The flattening of the pressure profile reduces the Shafranov shift resulting in an inward (to hfs) shift of the magnetic axis of about (a) 5 mm and (b) 10 mm and a corresponding decrease (sign definition by geometry and sign of current) of the angle due to an increased poloidal magnetic field at measurement position. The SC induced redistribution of the current results in a reduced poloidal magnetic field close to the plasma center and, hence, an increase in the angle. Close to the axis the effect from the current redistribution exceeds the one from the inward shift whereas at mid-radius the inward shift causes the dominant effect. A detailed study of the various effects including the redistribution of the fast particles is in progress.

This work has been carried out within the framework of the EUROfusion Consortium and has received funding from the Euratom research and training programme 2014-2018 under grant agreement No 633053. The views and opinions expressed herein do not necessarily reflect those of the European Commission.

References

[1] L. Giannone, B. Geiger, R. Bilato, M. Maraschek, T. Odstrcily, R. Fischer, P.J. McCarthy, J.C. Fuchs, V. Mertens, K.H. Schuhbeck, and ASDEX Upgrade Team. Real-time diamagnetic flux measurements on ASDEX Upgrade. *Rev. Sci. Instrum.*, 87:053509, 2016.

[2] R. Fischer, C.J. Fuchs, B. Kurzan, W. Suttrop, E. Wolfrum, and ASDEX Upgrade Team. Integrated data analysis of profile diagnostics at ASDEX Upgrade. *Fusion Sci. Technol.*, 58:675–684, 2010.

[3] S.K. Rathgeber, R. Fischer, S. Fietz, J. Hobirk, A. Kallenbach, H. Meister, T. Pütterich, F. Ryter, G. Tardini, E.Wolfrum, and the ASDEX Upgrade Team. Estimation of profiles of the effective ion charge at ASDEX Upgrade with Integrated Data Analysis. *Plasma Phys. Control. Fusion*, 52:095008, 2010.

[4] M. Weiland. *Influence of RF heating and MHD instabilities on the fast-ion distribution in ASDEX Upgrade*. PhD thesis, LMU München, 2016.

[5] R. Fischer, J. Hobirk, L. Barrera, A. Bock, A. Burckhart, I. Classen, M. Dunne, J.C. Fuchs, L. Giannone, K. Lackner, P.J. McCarthy, E. Poli, R. Preuss, M. Rampp, S.K. Rathgeber, M. Reich, B. Sieglin, W. Suttrop, E. Wolfrum, and ASDEX Upgrade Team. Magnetic equilibrium reconstruction using geometric information from temperature measurements at ASDEX Upgrade. In V. Naulin, C. Angioni, and M. Borghesi et al., editors, *40th EPS Conference on Plasma Physics*, volume 37D, page P2.139. European Physical Society, Geneva, 2013.

[6] O.P. Ford, A. Burckhart, R. McDermott, V. Igochine, R. Wolf, and JET EFDA Contributors. Imaging motional stark effect measurements at ASDEX Upgrade. In *21st Topical Conference on High Temperature Plasma Diagnostics (HTPD 2016)*, 2016.

[7] A. Mlynek, R. Fischer, O. Ford, P. Lang, B. Plöckl, and ASDEX Upgrade Team. First results from the new sub-millimeter polarimeter on the ASDEX Upgrade tokamak. In *21st Topical Conference on High Temperature Plasma Diagnostics (HTPD 2016)*, 2016.

[8] R. Fischer, A. Bock, M. Dunne, J.C. Fuchs, L. Giannone, K. Lackner, P.J. McCarthy, E. Poli, R. Preuss, M. Rampp, M. Schubert, J. Stober, W. Suttrop, G. Tardini, M. Weiland, and ASDEX Upgrade Team. Coupling of the flux diffusion equation with the equilibrium reconstruction at ASDEX Upgrade. *Fusion Sci. Technol.*, 69:526–536, 2016.

[9] V. Igochine, O. Dumbrajs, H. Zohm, A. Flaws, and the ASDEX Upgrade Team. Stochastic sawtooth reconnection in ASDEX Upgrade. *Nucl. Fusion*, 47:23–32, 2007.